CLM - P 75

United Kingdom Atomic Energy Authority

RESEARCH GROUP

Preprint

A MEASUREMENT OF THE CROSS SECTION FOR PRODUCTION OF $He^+(2S)$ IONS BY ELECTRON IMPACT EXCITATION OF GROUND STATE HELIUM IONS

D. F. DANCE
M. F. A. HARRISON
A. C. H. SMITH

Culham Laboratory,

Culham, Abingdon, Berkshire

1965

UNCLASSIFIED
(Approved for publication)

CLM - P 75

A MEASUREMENT OF THE CROSS SECTION FOR PRODUCTION OF $He^+(2S)$ IONS BY ELECTRON IMPACT EXCITATION OF GROUND STATE HELIUM IONS

by

D.F. DANCE
M.F.A. HARRISON
A.C.H. SMITH

(Submitted for publication in Proc. Roy. Soc.)

A B S T R A C T

A crossed beams method has been used to measure the cross section for the production of $He^+(2S)$ by electrons incident upon $He^+(1S)$ in the energy range from threshold to 750 eV. The cross section was measured in arbitrary units with an accuracy of ± 5% and at the higher energies its energy dependence is in close agreement with that calculated using the plane-wave Born approximation. Consequently, the cross section has been normalised to the plane-wave Born cross section at energies between 435 eV and 750 eV to obtain the absolute magnitude. An independent estimate of the absolute magnitude was made to within ± 30% using only the experimental parameters, and the absolute cross sections given by the two methods agree within the experimental uncertainties. The normalised cross section is compared with cross sections given by the close-coupling approximation and various Coulomb-Born approximations. At the lower energies the normalised cross section is considerably smaller than any of the theoretical values, but the measurements are consistent with the existence of a finite cross section at threshold if the energy spread of the electron beam is taken into account.

U.K.A.E.A. Research Group,
Culham Laboratory,
Nr. Abingdon,
Berks.

April, 1965 (C/18 ED)

C O N T E N T S

1. INTRODUCTION

Simple classical arguments such as those given by Seaton (1962) suggest that the cross sections for electron impact excitation of corresponding transitions in atoms and ions do not have the same dependence upon incident electron energy. The difference arises because an electron colliding with an ion gains kinetic energy from the long range Coulomb field of the ion and is most marked at energies close to the threshold. A finite excitation cross section of an ion at the threshold is a consequence of this increased energy. A similar argument predicts that the cross section for excitation of an atom is vanishingly small at threshold. At increasing electron energies the ionic field has progressively less effect so that the cross sections for ions tend to vary with energy in a manner similar to atoms.

The most extensive theoretical studies of excitation of ions by electron impact have been for the hydrogenic species such as He^+. Born's approximation, modified to take into account the Coulomb field, has been used by Tully (1960) to calculate the excitation cross section for He^+ ($1S \rightarrow 2S$), by Burgess (1961) for He^+ ($1S \rightarrow 2P$) and by Hummer (1963) for both He^+ ($1S \rightarrow 2S$) and He^+ ($1S \rightarrow 2P$). Application of the Bethe approximation to ($1S \rightarrow 2P$) excitation has been discussed by Seaton (1962). Burgess, Hummer and Tully (1963) have extended the Coulomb-Born calculations for both He^+ ($1S \rightarrow 2P$) and He^+ ($1S \rightarrow 2S$) to include some degree of coupling between the 1S, 2S and 2P states. They have also used the Coulomb-Born-Oppenheimer approximation to account for electron exchange. Burke, McVicar and Smith (1964a) have applied the close-coupling approximation to the calculation of the same cross sections. Their calculation allows for coupling between the 1S, 2S and 2P states and also takes into account electron exchange. This method contains fewer approximations and should give results of greater accuracy.

Cross sections calculated by means of the Coulomb-Born approximation and the close-coupling approximation are similar at energies above about twice the threshold, and at still greater energies they tend to the cross section given by the plane-wave Born approximation. At energies lower than twice the threshold, the close-coupling approximation yields relatively larger cross sections which are especially evident for the He^+ ($1S \rightarrow 2S$) transition. Consequently, a measurement of this cross section provides a particularly sensitive test of the theoretical methods.

No measurements of the excitation cross sections of ions have so far been reported. However, the development of a sensitive detector for He^+ ions in the metastable $2^2S_{\frac{1}{2}}$ state (Harrison, Dance, Dolder and Smith 1965; henceforth referred to as paper 1) has made it

possible to use a crossed beams technique to measure the cross section for the production of $He^+(2S)$ in collisions between electrons and ground state He^+ ions. The present paper describes the measurement of this cross section over the energy range 30 eV to 750 eV. This experiment could not distinguish $He^+(2S)$ ions formed by direct excitation from those formed by cascading from more highly excited states, but an estimate has been made of this cascade contribution so that the measured cross section could be compared with cross sections calculated for direct excitation.

2. THE EXPERIMENTAL METHOD

The crossed electron and ion beams technique has been described by Dolder, Harrison and Thonemann (1961). In this present experiment, $He^+(2S)$ ions produced by collisions between an electron beam and a 5 keV beam of ground state He^+ ions were detected 10^{-7} seconds after leaving the region where the beams crossed. These metastable ions were detected by counting the 40.8 eV photons which were emitted by $2^2P_{\frac{1}{2}} \rightarrow 1^2S_{\frac{1}{2}}$ transitions stimulated by Stark-effect mixing of the $2^2S_{\frac{1}{2}}$ and $2^2P_{\frac{1}{2}}$ states in a static electric field. Lamb and Skinner (1950) have calculated that the quenching action of an electric field of U [volts/cm] reduces the lifetime t [seconds] of the $2^2S_{\frac{1}{2}}$ state from 2.2×10^{-3} seconds to

$$t = 1.6 \times 10^{-2}/U^2, \qquad \ldots (1)$$

and so the metastable ions could be effectively quenched in an electric field of a few thousand volts per centimetre.

Ground state ions were excited to all energetically accessible states by collisions with the electron beam. Photons emitted by the decay of readily-excited states, other than the $2^2S_{\frac{1}{2}}$, were not observed because the lifetimes of such states are shorter than the 10^{-7} seconds taken by the ions to travel from the collision region to the detector. For example, the $2^2P_{\frac{1}{2}}$ state has a lifetime of 10^{-10} seconds. The number of ions excited to long-lived highly-excited states was insignificant because the cross sections for these excitations are relatively much smaller. Depopulation of the $2^2S_{\frac{1}{2}}$ state between the collision region and detector was negligible because the lifetime for natural decay of the state is long compared with 10^{-7} seconds. In addition, the residual gas pressure (10^{-8} torr) was too low for appreciable collisional de-excitation to occur. Consequently, virtually all the He^+ ions excited by electron collisions decayed to the ground state or to the $2^2S_{\frac{1}{2}}$ state before entering the detector, and so the cross section measured was that for the production of $He^+(2S)$ and included cascade contributions from more highly excited states.

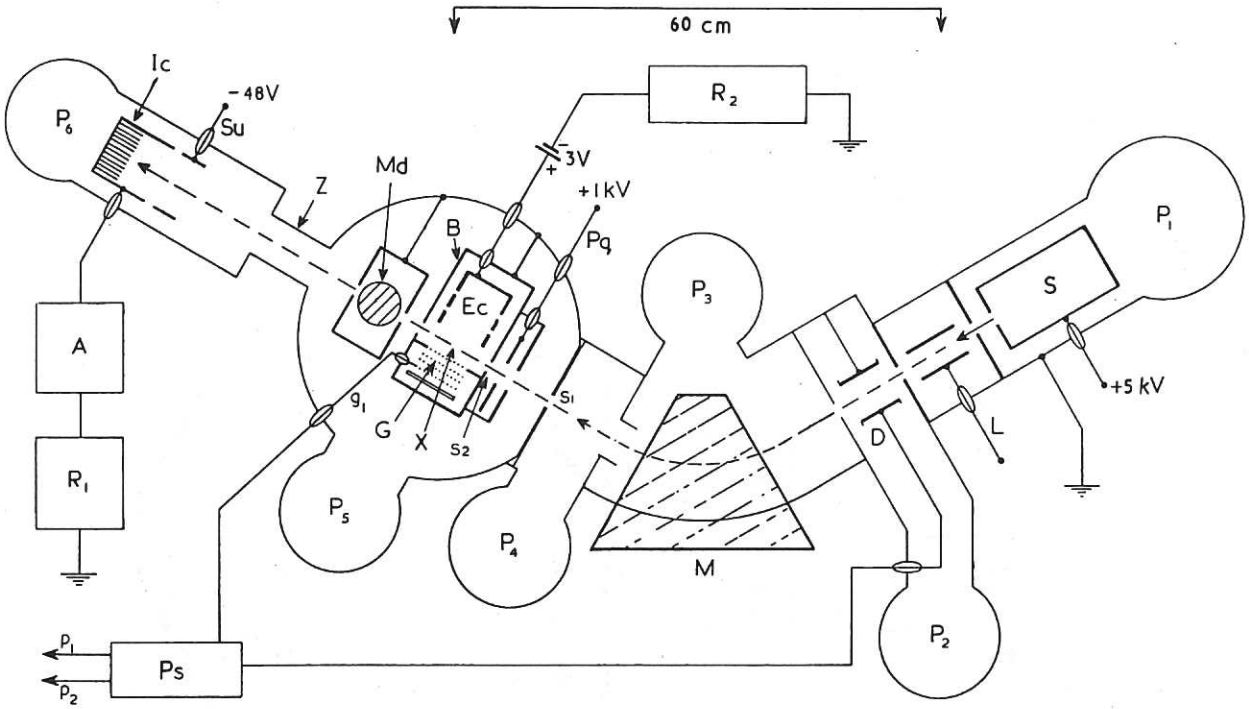

Fig. 1 (CLM-P 75)

Schematic plan view of the apparatus. S, ion source; L, einzel lens; D, deflector plate for pulsing the ion beam; M, electromagnet; s_1 and s_2, collimating slits; P_q, pre-quench electrode; X, collision region; B, magnetic shield for the electron gun G; g_1, control grid of the electron gun; Ec, electron collector; Md, $He^+(2S)$ ion detector; Z, impedance; Ic, ion collector; Su, secondary electron suppressor; A, d.c. amplifier; R_1 and R_2, recorders; P_1 to P_6, diffusion pumps; Ps, pulse generator; p_1 and p_2, gating pulses for scalers (see Fig. 3)

3. THE APPARATUS

The apparatus is shown schematically in Fig. 1. Ions from an oscillatory-electron type ion source S were accelerated to the einzel lens L and passed through a 60^o sector magnet M so that a focussed 5 keV beam of He^+ ions, 0.2 cm in height and 0.1 cm wide, was defined by the collimator slits s_1 and s_2. The collimated ion beam traversed the collision region X where it was crossed at right angles by an electron beam passing

from the gun G to the electron collector Ec. These are shown in more detail in Fig.2. The width of the electron beam was 2.5 cm and its height was restricted in the gun so that only those electrons which passed through the ion beam were collected. After leaving the collision region, the ion beam travelled a further 5 cm before entering the metastable $He^+(2S)$ ion detector Md. The beam was finally collected in the Faraday cup Ic. A modulated beams technique was used so that $He^+(2S)$ ions formed by collisions between the two beams could be distinguished from backgrounds due to various conflicting processes. Both beams were pulsed on and off in the sequence described in Section 4 by applying suitable potentials to the control grid g_1 of the electron gun and to the ion beam deflector plate D.

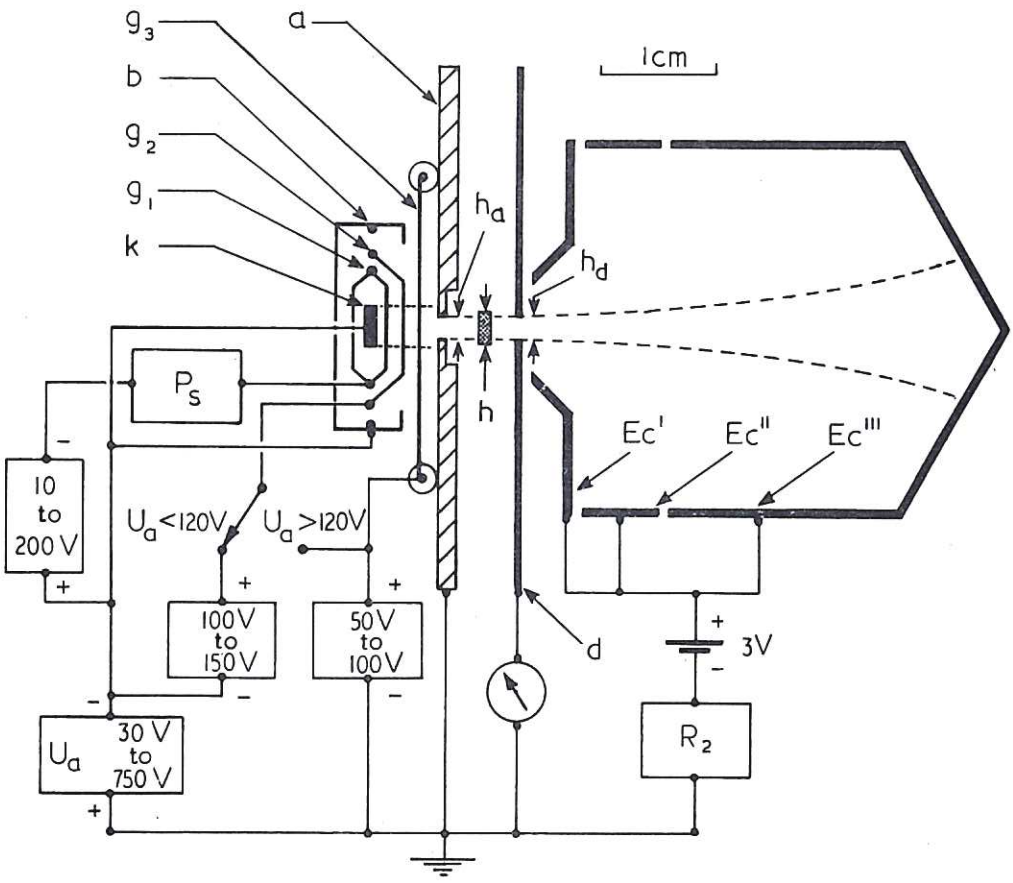

Fig. 2 (CLM-P75)

Electron gun and collector viewed along the axis of the ion beam. k, cathode; g_1, control grid; g_2, accelerating grid; b, beam focussing plates; g_3, suppressor grid. g_2 and g_3 were always biased positively relative to the anode a so that secondary electrons formed at a, g_2 and g_3 could not enter the collision region. The height h of the ion beam was 0.2 cm. The electron beam was restricted at the anode to a height of h_a = 0.16 cm and was focussed so that a negligible current was collected at the aperture of height h_d = 0.19 cm in the plate d. The Faraday cup electron collector consisted of electrodes Ec′, Ec″ and Ec‴. Field penetration into the collision region was measured for a model in an electrolytic tank and was found to give rise to a potential of less than 0.1 volts

The $He^+(2S)$ ion detector described in paper 1 is shown in a simplified form in Fig.3. Ions entered through the tube T_1, which was at earth potential, and were accelerated in the field produced by biasing the concentric quench tube T_2 to -1400 volts. This field quenched over 90% of the $He^+(2S)$ ions, and the resulting photons, which were emitted isotropically (Lichten 1961), passed through the grids in the tubes T_1 and T_2 and also in a third tube T_3. The latter tube was earthed and so it shielded the photocathodes Pc_1 and Pc_2 from the potential applied to T_2. The photocathodes encircled T_3, and Pc_1 was biased to +300 volts so that, in addition to incident photons, it detected photoelectrons accelerated from Pc_2. Electrons emitted from Pc_1 were detected by a 17-stage electron multiplier Mu (E.M.I. type 9643). The grids in T_2 and T_3 were covered with aluminium films 1000 Å in thickness. These films, which were each about 45% transparent to 40.8 eV photons, shielded the photocathodes from charged particles. The potential applied to T_2 was always negative so that stray electrons were repelled from the detector.

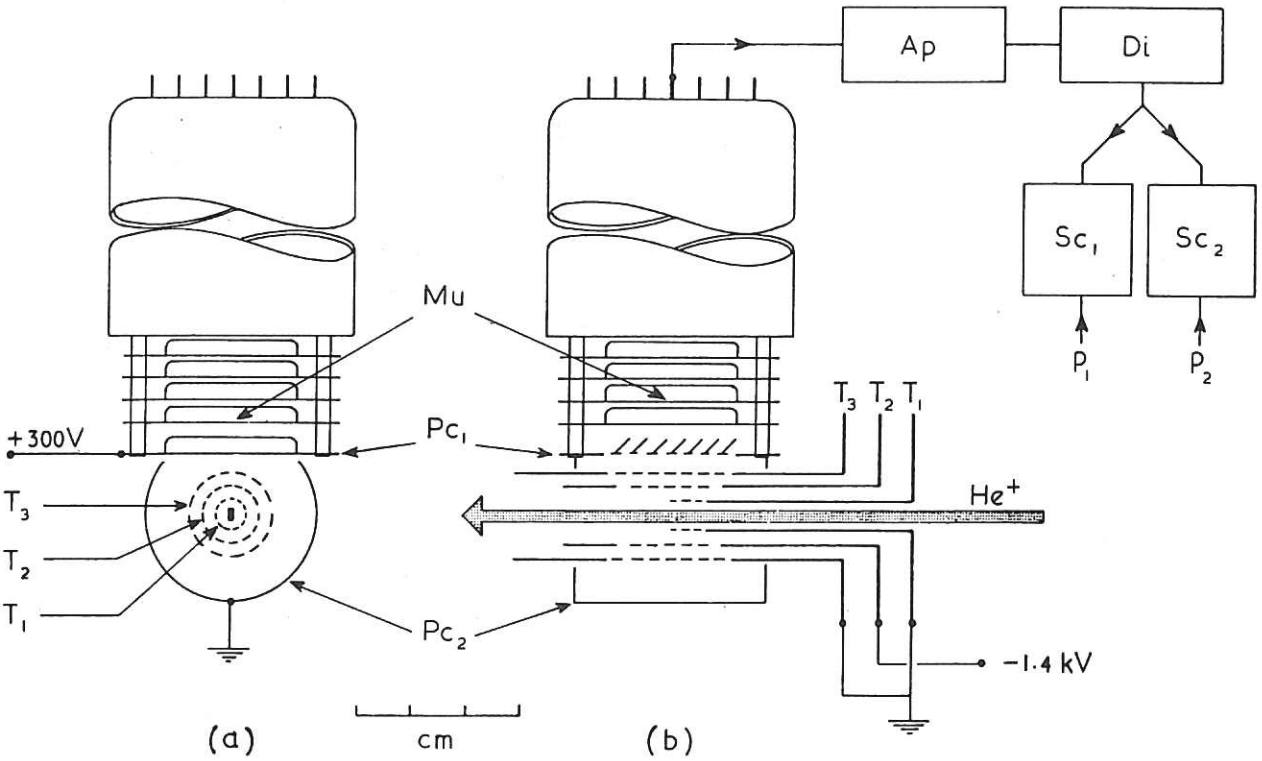

Fig. 3 (CLM-P75)
Schematic diagrams of the end view (a) and side view (b) of the $He^+(2S)$ ion detector. T_1, ion beam entry tube; T_2, quench tube; T_3, shield for photocathodes; Pc_1, venetian blind photocathode; Pc_2, saddle-shaped photocathode; Mu, electron multiplier (E.M.I. 9643); Ap, pulse amplifier; Di, discriminator; Sc_1 and Sc_2, scalers gated by pulses p_1 and p_2. The grids in T_2 and T_3 were covered with aluminium films 1000 Å in thickness

The photomultiplier assembly was operated as a single photon detector. Its output pulses were amplified and, after suitable discrimination against electronic noise, were fed to two scalers whose inputs were connected in parallel. The scalers were gated so that their counting periods were synchronised to the beams pulsing sequence.

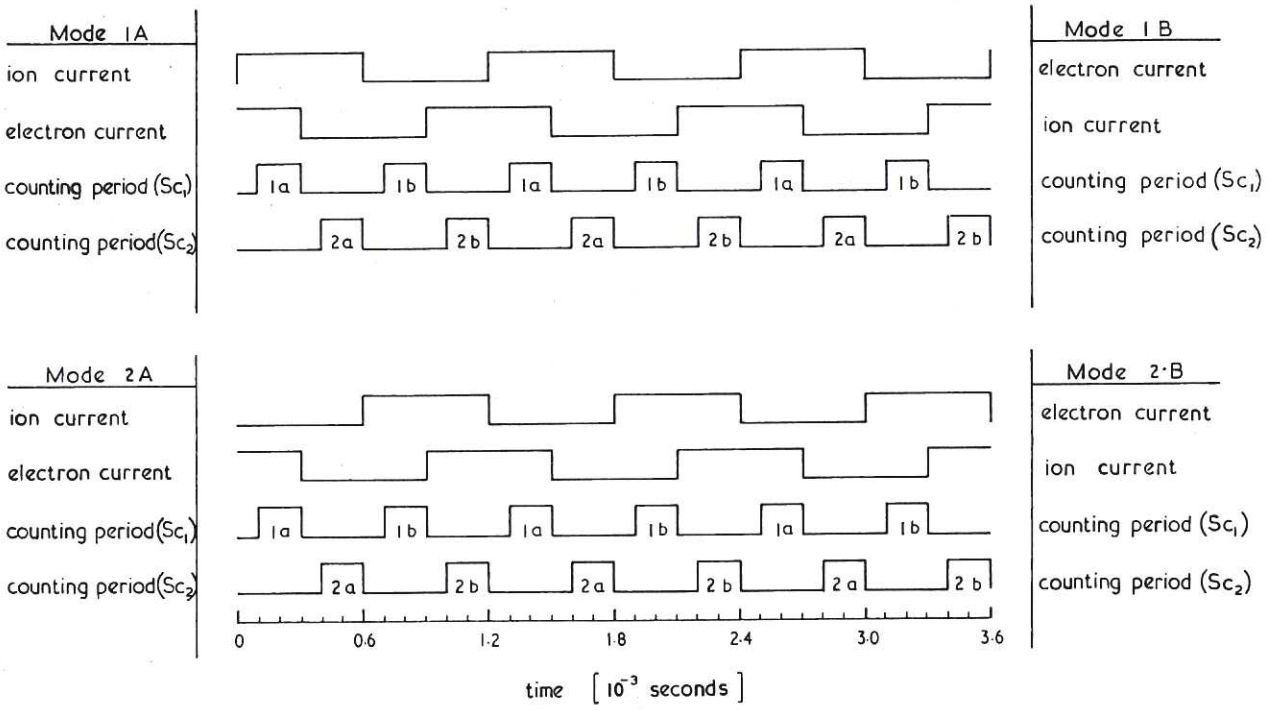

Fig. 4 (CLM-P 75)
Waveforms of the sequence of pulsed beams and scaler counting periods used to separate the signal from electron and ion backgrounds. The signal was measured in counting periods 1a for modes 1A and 1B and in periods 2b for modes 2A and 2B. The pulsing sequence was automatically changed from mode 1A to mode 1B or from mode 2A to mode 2B at every 50th pulse of ion current

4. MEASUREMENT OF THE SIGNAL

The signal is defined as the count rate produced by the interaction of the electron and ion beams. It was found that each beam gave rise to a background count rate, and the signal was distinguished from these backgrounds by means of the pulsing sequence shown in Fig.4. The ion beam was pulsed on and off with a pulse duration of 600 microseconds and a duty cycle of 50%. The electron beam was similarly pulsed but phased to cut off half way through the ion beam pulse. Gating pulses of 200 microseconds duration were applied to the scalers and were so phased that in mode 1A scaler Sc_1 counted in period 1a when both beams were pulsed on and also in period 1b when both beams were pulsed off. Scaler Sc_2 counted in period 2a when the ion beam alone was pulsed on and also in period 2b when the electron beam alone was pulsed on. If B_e and B_i are respectively the background count

rates produced by the electron beam and the ion beam, B_d is the count rate due to electronic noise and C_c is the signal, then

$$\text{scaler } Sc_1 \text{ measured } \left[C_c + B_i + B_e + B_d\right]_{1a} + \left[B_d\right]_{1b}$$

$$\text{and scaler } Sc_2 \text{ measured } \left[B_i + B_d\right]_{2a} + \left[B_e + B_d\right]_{2b} ,$$

where the subscripts outside the brackets refer to the appropriate counting period. Thus the difference between the readings of scalers Sc_1 and Sc_2 gave the signal C_c.

In mode 1A scaler Sc_1 counted for part of the first half of the ion beam pulse and for part of the second half of the electron beam pulse. Scaler Sc_2 counted vice versa and so an error would have been introduced if the background produced by either the electron or ion beam varied systematically during the pulses. The backgrounds were proportional to the beam currents (see Section 6) and a systematic variation of the electron current during the pulses was observed for certain operating conditions. Similar variations of the ion beam current pulses were not detected, but the background produced by this beam was sensitive to any small systematic changes of pressure (see Section 6). In order to overcome these sources of error, the phases of the ion and electron beam pulses could be interchanged (mode 1B). In this mode the signal was still recorded in scaler Sc_1, which now counted in the second half of the ion beam pulse and in the first half of the electron beam pulse, while scaler Sc_2 again counted vice versa. The pulsing sequence was automatically alternated between mode 1A and mode 1B at a rate corresponding to every 50th ion beam pulse so that the signals were automatically averaged over the first and second halves of the beam pulses.

In modes 2A and 2B the ion beam pulse was delayed for 600 microseconds so that the signal was recorded in counting period 2b of scaler Sc_2. Inequalities between the first and second halves of the beam pulses were again eliminated by alternating automatically between modes 2A and 2B. Thus any inequalities in the scalers or their counting periods could be eliminated by measuring the signal for equal times in modes 1 and 2 and taking the average.

The pulsing sequence was derived from a crystal controlled oscillator and the stability of the complete system was adequate to measure the signal to an accuracy of one part in 10^4 of the background count rate, provided that the total number of counts recorded was sufficient to give statistical significance.

Measurements were made in the following manner. At a particular electron energy E and beam current J, the pulsing sequence was run in modes 1A and 1B for 180 seconds and

the difference between the readings of scalers Sc_1 and Sc_2 was recorded at the end of this period. The pulsing sequence was then changed to modes 2A and 2B. A total of eight observations of the difference between the scalers was taken alternately in modes 1 and 2 and the signal $C_c(E)$ was calculated from their average.

5. DETERMINATION OF THE CROSS SECTION

The fraction ε of the $He^+(2S)$ ion beam entering the detector system which gave rise to output pulses recorded by the scalers has been estimated in paper 1 to be $\varepsilon = (8.3 \pm 2.5)\ 10^{-3}$. In view of the uncertainty in the efficiency of the detector, the principal objective of the experiment has been to measure accurately $Q_d(E)$, which is the cross section for the production of detected $He^+(2S)$ ions arising from collisions between electrons with incident energy E and ground state He^+ ions. The absolute cross section $Q_p(E)$ for the production of $He^+(2S)$ is related to $Q_d(E)$ by

$$Q_p^e(E) = \frac{1}{\varepsilon} Q_d(E) , \qquad \ldots (2)$$

where the superscript e denotes an experimental determination.

The cross section $Q_d(E)$ was determined in the manner discussed by Harrison (1965; henceforth referred to as paper 2) from the following expression:

$$Q_d(E) = \frac{C(E)}{IJ} \frac{e^2 h v V}{(v^2 + V^2)^{\frac{1}{2}}} F, \qquad \ldots (3)$$

where

$$E = \tfrac{1}{2}m(v^2 + V^2) . \qquad \ldots (4)$$

Here, $C(E)$ is the detected count rate due to the production of $He^+(2S)$ ions by collisions between the ion and electron beams, and I and J are respectively the total beam currents of ions and electrons which cross the collision region with velocities V and v; the electronic mass and charge are respectively m and e, and h is the height of the ion beam. The factor F takes account of inhomogeneities in beam particle densities and was estimated, as described in paper 2, from measurements of the current density profiles of each beam. Adjustment of the apparatus always ensured that $0.98 < F < 1.00$.

Ion and electron beam space charge caused the signal $C_c(E)$, measured as described in Section 4, to differ from $C(E)$ by an amount proportional to IJ. This difference is discussed in Section 7. Excessive electron space charge could also cause a non-linear relationship between $C_c(E)$ and IJ (discussed further in paper 2), but the electron beam density was limited so that this effect did not occur. The proportionality of $C_c(E)$

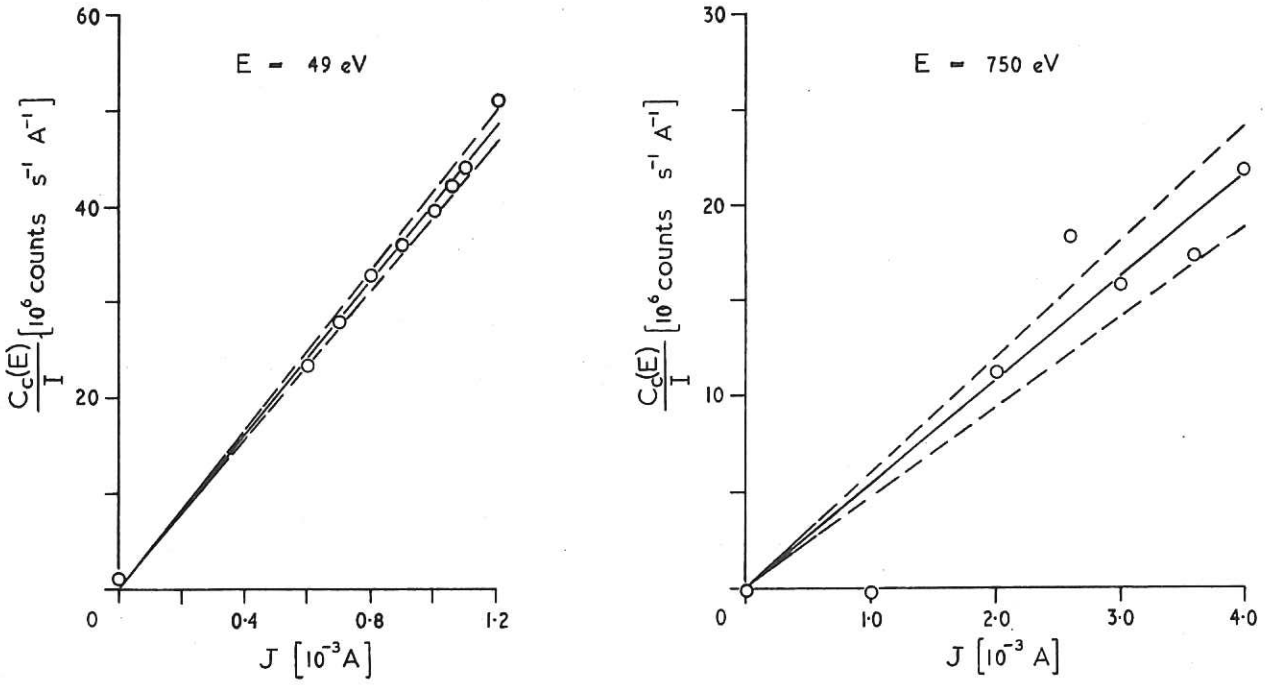

Fig. 5 (CLM-P 75)

Relationship between $C_c(E)/I$ and the electron beam current J measured for two electron energies. Signals $C_c(E)$ were measured at ion currents I of about 10^{-6} A and the currents and count rates refer to the instantaneous values during the beam pulses. The broken lines indicate the 90% confidence limits of the slopes

to IJ is demonstrated in Fig.5 where typical results for $C_c(E)/I$ are shown plotted against J at electron energies E = 49 eV and 750 eV. The solid straight line through the origin was fitted to the points by the method of least squares. The implied assumption that $C_c(E)/I = 0$ for $J = 0$ was closely in agreement with the average value for $J = 0$ measured at a number of electron energies. The broken lines show 90% confidence limits of the slope. They were determined in the manner described by Acton (1959). A correction for space charge effects, as described in Section 7, was applied to the slope for each electron energy and the value of the corrected slope was substituted for the factor C(E)/IJ in equation (3) to yield the value of $Q_d(E)$. Typical instantaneous values of these parameters were $I = 10^{-6}$A, J = 4mA (maximum) and the maximum value of C(E) was about 70 counts per second.

6. BACKGROUNDS

The metastable ion detector responded in some measure to photons with energies ranging from about 15 eV to several hundred electron volts. The ion and electron beams

independently gave rise to photons within this bandwidth and these were the cause of the backgrounds mentioned in Section 3 and Section 4. Collisions with the electron beam excited fewer than one in 10^9 of the incident ground state helium ions to the 2S state, and the count rate registered by the scalers due to the quenching of these ions was much smaller than the background count rate produced by either of the two beams separately. An additional but much smaller background due to electronic noise was observed when neither beam was present. The principal backgrounds were attributed to (a) metastable helium ions formed in the ion source, (b) collisions between ground state helium ions and residual gas and (c) collisions of electrons with surfaces in the electron gun and collector. These phenomena are discussed below.

(a) Metastable helium ions produced in the ion source

Excited ions which emanated from the ion source and entered the $He^+(2S)$ ion detector must have been in the metastable 2S state because the radiative lifetimes of other likely excited states were many orders shorter than the ion transit time. Relatively large numbers of metastable ions reached the detector despite the combined quenching actions of the ion extraction field and the Lorentz field of the magnet M. The background caused by these ions was virtually eliminated by restricting the energy of electrons in the ion source to less than the threshold energy (65.4 eV) for the direct excitation of ground state helium atoms to the 2S state of He^+.

(b) Collisions between ground state He^+ ions and residual gas

When excited ions from the ion source were eliminated, the remaining background arising from the ion beam was found to be proportional to the ion beam current and also dependent upon pressure. This background was mainly due to photons produced in collisions between ions and gas atoms near the detector. Ionizing collisions in the negative potential region inside the quench tube T_2 may have contributed because free electrons from these collisions could produce detectable bremsstrahlung photons when they struck nearby earthed electrodes. In addition, $He^+(2S)$ ions were produced by excitation of the $He^+(1S)$ beam in collisions with residual gas between M and the detector. The background from these ions was reduced by biasing to +1000 volts the pre-quench electrode Pq located in front of the collision region.

The pressure near the detector depended upon the amount of gas which effused from the ion source. This was reduced to an acceptable value of about 10^{-8} torr by interposing four stages of differential pumping between the ion source and the collimating slit S_2.

Further precautions were taken by pulsing the ion beam near the ion source so that gas formed by neutralisation of the He^+ beam, when it was cut off, was pumped away by the early differential stages. In addition, an impedance Z was interposed between the ion collector Ic and the $He^+(2S)$ ion detector Md so that backstreaming of neutralised ions was reduced. As a result of the various precautions outlined here and in (a), the background arising from the ion beam was reduced to about ten times the maximum count rate caused by collisions between the two beams.

(c) Collisions of electrons with surfaces

The background produced by the electron beam was proportional to electron energy and current. It was about 50 times greater than the count rate produced by collisions between the ion beam and a 750 eV electron beam. This background did not depend upon pressure and was only slightly affected by large changes in the potential applied to the quench tube T_2. Consequently, it was not due to electron impact excitation of residual gas and was unlikely to have been caused by electrons from the gun entering the quench region. The most likely cause of this background was bremsstrahlung photons which were produced by collisions of electrons with surfaces in the electron gun and collector and were subsequently reflected into the $He^+(2S)$ detector. It would appear from the geometry of the apparatus that this background arose predominantly from a small fraction of the electron beam which struck the plate d located in front of the electron collector (see Fig.2).

7. CORRECTIONS FOR SPACE CHARGE MODULATION OF THE BACKGROUNDS

Signals were observed at all energies below 40.8 eV, which is the threshold for excitation to the 2S state of He^+. These were typically 10% of the maximum signals observed at energies above the threshold and could not be accounted for by the electron energy spread. The signals observed above the threshold were therefore not solely due to the detection of $He^+(2S)$ ions produced by collisions between the two beams. This effect arose because the backgrounds present when the beams crossed were not quite equal to those measured for each beam on its own. These variations in the magnitude of the backgrounds were caused by the action of electron space charge upon the ion trajectories and of ion space charge upon the electron trajectories. The ion beam was slightly divergent so that a small fraction, less than 1%, was intercepted at the entrance to the $He^+(2S)$ ion detector. The ion trajectories were converged towards the axis of the ion beam when the electron beam was pulsed on so that a greater ion current passed through the detector and hence the ion background was increased. Convergence of the electron trajectories by the ion space charge decreased the

number of electrons striking the plate d in front of the electron collector, and so reduced the number of bremsstrahlung photons which could be reflected into the $He^+(2S)$ ion detector. Consequently, the electron background decreased when the ion beam was pulsed on. At an electron energy E, the signal could be expressed as

$$C_c(E) = C(E) + b_i(E) - b_e(E) \ , \qquad \ldots (5)$$

where C(E) is the count rate due to the production of $He^+(2S)$, and $b_i(E)$ and $b_e(E)$ are respectively the modulated components of the ion and electron backgrounds. These modulation effects are discussed in paper 2 where it is predicted that both components $b_i(E)$ and $b_e(E)$ are proportional to IJ. Thus the signal per unit beam currents was given by

$$C'_c(E) = C'(E) + b'_i(E) - b'_e(E) \ , \qquad \ldots (6)$$

where each term is equal to the corresponding term in equation (5) divided by IJ. The modulated components $b'_i(E)$ and $b'_e(E)$ could not be measured separately, but it was possible to measure their combined effect by reducing the quench potential to -50 volts so that insignificant numbers of $He^+(2S)$ ions were detected. Under these conditions C'(E) was zero and $\left\{C'_c(E)\right\}_q$, the signal per unit beam currents, was given by

$$\left\{C'_c(E)\right\}_q = \left\{b'_i(E)\right\}_q - \left\{b'_e(E)\right\}_q \ . \qquad \ldots (7)$$

Altering the quench potential caused a negligible change in the electron background and so $b'_e(E) = \left\{b'_e(E)\right\}_q$. The same was not true for the ion background (see Section 7b) and so $b'_i(E)$ was not equal to $\left\{b'_i(E)\right\}_q$. Consequently, the difference between the signals expressed by equations (6) and (7) yielded

$$C'(E) = C'_c(E) - \left\{C'_c(E)\right\}_q - \left(b'_i(E) - \left\{b'_i(E)\right\}_q \right) . \qquad \ldots (8)$$

It is shown in the following sections (a) and (b) that $\left(b'_i(E) - \left\{b'_i(E)\right\}_q\right)$ could be determined from measurements made with quench potentials of -1400 volts and -50 volts and, because $C'_c(E)$ and $\left\{C'_c(E)\right\}_q$ were measured quantities, C'(E) could thus be determined from equation (8).

(a) Measurements with a quench potential of -1400 volts

A simple theory presented in paper 2 of the effect of electron beam space charge on an ion beam indicates that

$$b'_i(E) = \frac{K}{E^{\frac{1}{2}}} \ , \qquad \ldots (9)$$

where K is a constant which depends on the ion beam energy and the geometry of the apparatus. Thus, from equation (6),

$$C'_c(E) = C'(E) + \frac{K}{E^{\frac{1}{2}}} - b'_e(E) \quad . \qquad \ldots (10)$$

One of the factors on which K depended was the angular deviation of the ion beam from the geometrical axis of the collision region and entrance tube T_1 of the $He^+(2S)$ ion detector. When the alignment of the ion beam was varied mechanically by about 0.2^o, the maximum signal above threshold was found to change by about 15%. This adjustment did not move the detector relative to the electron gun and so the change in signal was unlikely to have been caused by a change in the electron background. Therefore the difference between the signals measured at the same electron energy but for different alignments could be expressed by equations of the type

$$\left\{C_c(E)\right\}_1 - \left\{C_c(E)\right\}_m = \frac{K_1 - K_m}{E^{\frac{1}{2}}} \quad \text{etc.}, \qquad \ldots (11)$$

where the subscripts 1, m, etc. refer to the different alignments. The signals for four different alignments were measured at electron energies ranging from 30 eV to 750 eV and two of the differences, $\left\{C_c(E)\right\}_1 - \left\{C_c(E)\right\}_m$ etc., are plotted against $E^{-\frac{1}{2}}$ in Fig.6. These results demonstrate that the modulated component of ion background varied as $E^{-\frac{1}{2}}$

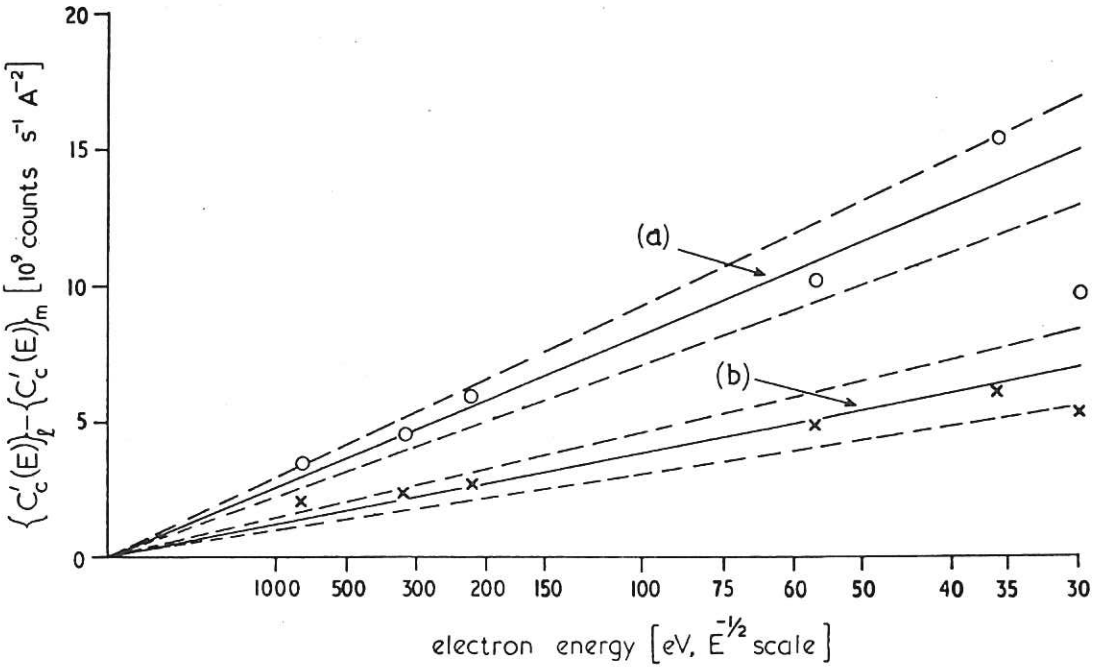

Fig. 6 (CLM-P75)
The difference $\{C'_c(E)\}_l - \{C'_c(E)\}_m$ plotted against $E^{-\frac{1}{2}}$. Two sets of differences are shown by the lines (a) and (b). The broken lines represent the 90% confidence limits of the slopes $(K_l - K_m)$

over the complete energy range. In order to increase the statistical significance of the measured values of $\left\{C'_c(E)\right\}_1$ etc., the four sets of measurements were combined by using the slopes $(K_1 - K_m)$ etc. to correct each set to a common value of $b'_i(E)$, so that the corrected value $\left\{C'_c(E)\right\}_o$ is given by

$$\left\{C'(E)\right\}_o = C'(E) + \frac{K_o}{E^{\frac{1}{2}}} - b'_e(E) \qquad \ldots (12)$$

(b) Measurements with a quench potential of -50 volts

It was expected that $\left\{b'_i(E)\right\}_q$ would differ from $b'_i(E)$ because the reduction in quench potential would alter the ion trajectories and also reduce the number of collision processes which could contribute to the background. However, this would not alter the energy dependence and so $\left\{C'_c(E)\right\}_q$ could be expressed as

$$\left\{C'_c(E)\right\}_q = \frac{K_q}{E^{\frac{1}{2}}} - b'_e(E) \qquad \ldots (13)$$

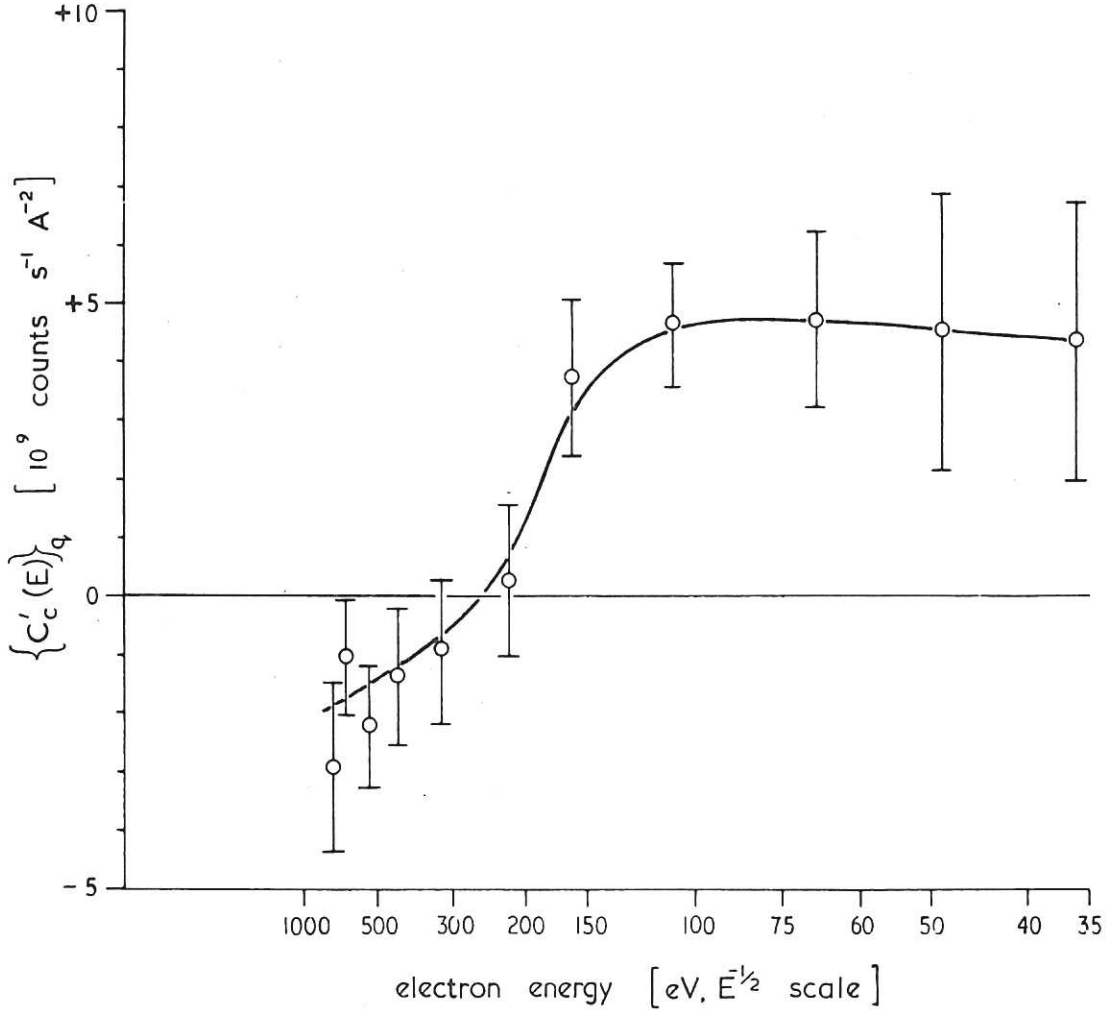

Fig. 7 (CLM-P 75)
$\{C'_c(E)\}_q$ measured for a quench potential of -50 volts and plotted against $E^{-\frac{1}{2}}$. A smooth curve is drawn through the experimental points and the brackets show the 90% confidence limits of the points

Measurements of $\left\{C_c'(E)\right\}_q$ were made at electron energies between 36 eV and 750 eV and are shown plotted against $E^{-\frac{1}{2}}$ in Fig.7. The results do not lie on a straight line through the origin and therefore they demonstrate the existence of $b_e'(E)$. The observed energy dependence of $\left\{C_c'(E)\right\}_q$ is discussed in paper 2 where it is shown that this dependence is not unreasonable in view of the assumption that $b_e'(E)$ was caused by the effect of ion space charge on the electron beam in the collision region.

The difference between the signals expressed by equations (12) and (13) yielded

$$C'(E) = \left\{C_c'(E)\right\}_o - \left\{C_c'(E)\right\}_q - \frac{(K_o - K_q)}{E^{\frac{1}{2}}} . \qquad \ldots (14)$$

At energies below the 2S threshold, $C'(E)$ was zero and so $(K_o - K_q)$ was determined from the difference between the signals measured at 36 eV.

In Fig.8 the points show $C'(E)$ found from equation (14) and the brackets show 90% confidence limits at each energy. The magnitude of the overall corrections made to the

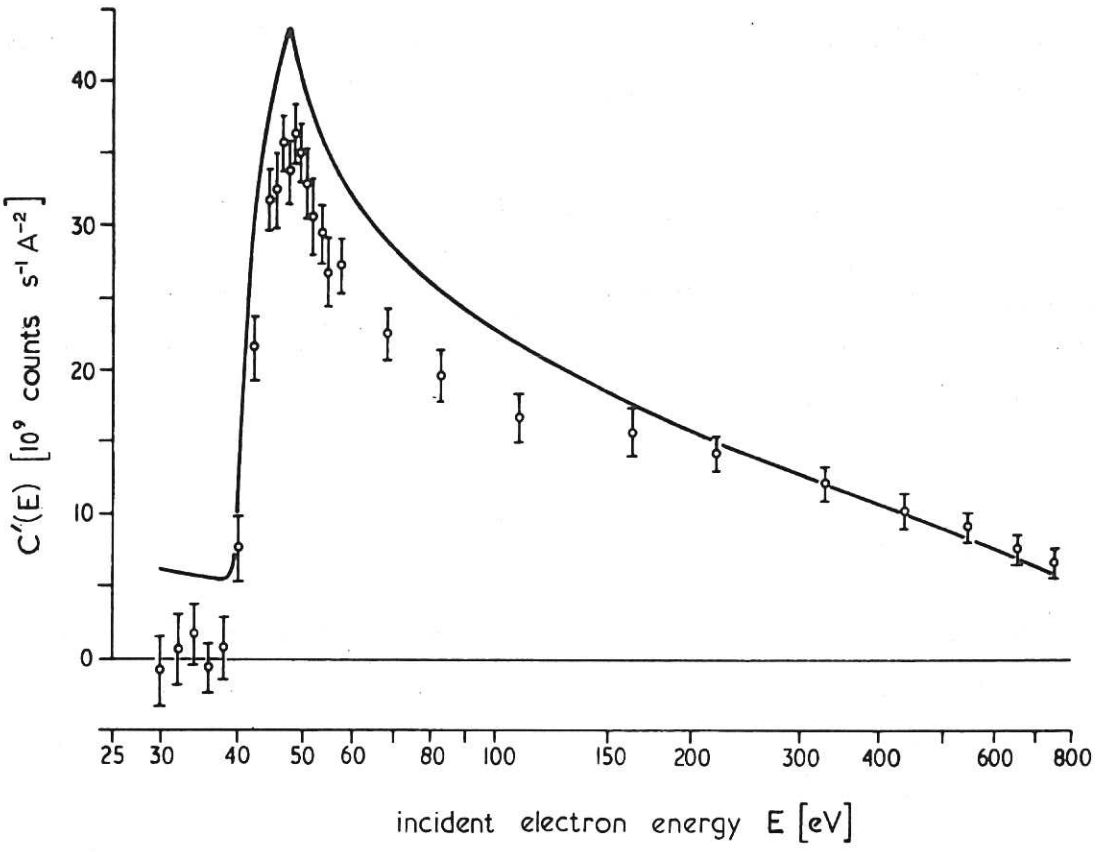

Fig. 8 (CLM-P 75)
Variation with electron energy E of the count rate due to the production of $He^+(2S)$. The points show $C'(E)$ given by equation (14) and the brackets represent 90% confidence limits. The magnitude of the corrections made to the experimental points is demonstrated by comparing them with the smooth curve, which was drawn through the uncorrected results for one alignment of the ion beam

experimental points is shown by their deviations from the smooth curve drawn through the uncorrected results for one alignment of the ion beam.

8. ESTIMATION OF CONTRIBUTIONS FROM CASCADE

The theoretical cross sections for direct excitation of $He^+(2S)$ discussed in Section 1 do not account for the population of the 2S state by cascading from more highly excited states. An estimate of these contributions is therefore required in order to compare the present experimental results with theory.

The cross section $Q_p(E)$ for the production of $He^+(2S)$ may be expressed as

$$Q_p(E) = Q_{1S \rightarrow 2S}(E) + Q_c(E) \ , \qquad \ldots (15)$$

where $Q_{1S \rightarrow 2S}(E)$ is the cross section for direct excitation of $He^+(2S)$ and $Q_c(E)$ is the cross section for contributions from cascade. The cascading is predominantly from the P states and so $Q_c(E)$ may approximated to

$$Q_c(E) \approx \sum_{n=3}^{\infty} \Upsilon_{nP \rightarrow 2S} \, Q_{1S \rightarrow nP}(E) \ . \qquad \ldots (16)$$

Here $\Upsilon_{nP \rightarrow 2S}$ is the branching ratio for $nP \rightarrow 2S$ transitions and $Q_{1S \rightarrow nP}(E)$ is the cross section for direct excitation to the nP state from the ground state. Lichten and Schultz (1959) have proposed a simplified expression for $Q_c(E)$, namely

$$Q_c(E) = 0.21 \, Q_{1S \rightarrow 3P}(E) \ . \qquad \ldots (17)$$

Hummer and Seaton (1961) suggest that $0.23 \, Q_{1S \rightarrow 3P}(E)$ is a more accurate approximation.

Burke, McVicar and Smith (1964b) have used the close-coupling approximation to calculate $Q^{cc}_{1S \rightarrow 3P}(E)$ at energies less than 68 eV. The cross section has not been calculated at higher energies, but nevertheless it can be assumed to vary with energy in a similar manner to $Q_{1S \rightarrow 2P}(E)$. This latter cross section has been calculated (see Section 1), but a comparison with the measurements for the same transition in atomic hydrogen made by Fite and Brackmann (1958a) indicates that Born-type approximations are likely to overestimate the cross section at energies less than about twenty times the threshold. This argument is supported by the energy dependence of $Q^e_i(E)$, which is the ionization cross section of He^+ measured by Dolder, Harrison and Thonemann (1961). The ionization cross section may well differ from theory in a manner similar to $Q_{1S \rightarrow 2P}(E)$ because a major

contribution to ionization arises from excitation to P states in the continuum. A semi-empirical cross section $Q^{s}_{1S \to 2P}(E)$ for direct excitation to the 2P state was therefore estimated from

$$Q^{s}_{1S \to 2P}(E) = Y(E)\ Q^{cb}_{1S \to 2P}(E) \ , \qquad \ldots (18)$$

where

$$Y(E) = \frac{Q^{e}_{i}(E')}{Q^{cb}_{i}(E')} \qquad \ldots (19)$$

and

$$E' = \frac{\chi}{E_2}\, E \ . \qquad \ldots (20)$$

The superscript cb refers to the Coulomb-Born calculations made by Burgess (1961) for ionization and for direct excitation to the 2P state. The ionization energy of He^{+} is χ and E_2 is the excitation energy of the 2P state. These Coulomb-Born calculations extend only to $E = 6\chi$, but they have been extrapolated to higher energies using the corresponding plane-wave Born cross sections for atomic hydrogen (Massey 1956) scaled by $(\chi_H/\chi)^2$, where χ_H is the ionization energy of atomic hydrogen.

Cross sections for direct excitation to other P states were calculated from $Q^{s}_{1S \to 2P}(E)$ by the following scaling procedure:

$$Q^{s}_{1S \to nP}(E) = T(E)\ Q^{s}_{1S \to 2P}(E'') \ , \qquad \ldots (21)$$

where

$$T(E) = \left[\frac{Q_{1S \to nP}(E_H)}{Q_{1S \to 2P}(E''_H)}\right]_{\text{atomic hydrogen}} , \qquad \ldots (22)$$

$$E'' = \frac{E_2}{E_n}\, E, \quad E_H = \frac{\chi_H}{\chi}\, E, \quad E''_H = \frac{\chi_H}{\chi}\, E'' \ , \qquad \ldots (23)$$

and E_n is the excitation energy of the nP state of He^{+}. The scaling factors T(E) were taken from the plane-wave Born cross sections for atomic hydrogen.

The final form of the semi-empirical cascade cross section is given in Fig.9 which shows $Q^{s}_{c}(E)$ calculated from

$$Q^{s}_{c}(E) = \Upsilon_{3P \to 2S}\ Q^{s}_{1S \to 3P}(E) + \Upsilon_{4P \to 2S}\ Q^{s}_{1S \to 4P}(E) \quad \left[E < E_5\right] \qquad \ldots (24a)$$

and

$$Q^{s}_{c}(E) = 0.23\ Q^{s}_{1S \to 3P}(E) \quad \left[E \geqslant E_5\right] \ . \qquad \ldots (24b)$$

The branching ratios, Υ, of He^{+} are the same as for the corresponding transitions in atomic hydrogen, and so the values of $\Upsilon_{np \to 2S}$ could be calculated from the transition probabilities of atomic hydrogen given by Condon and Shortley (1959).

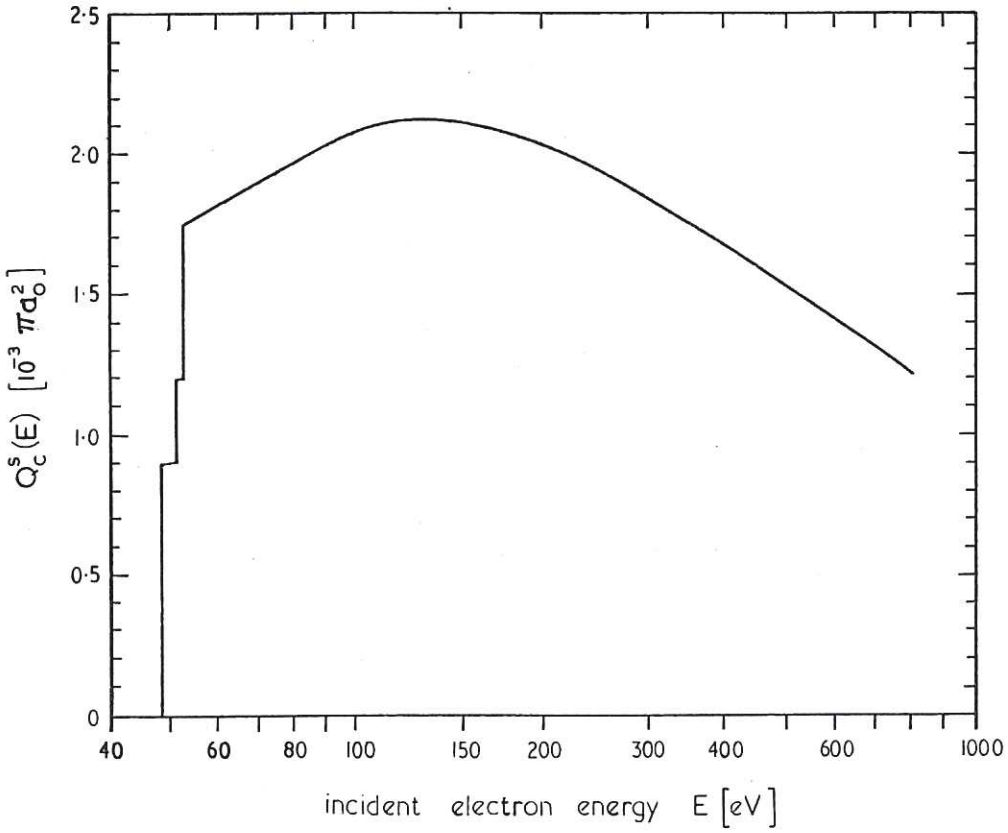

Fig. 9 (CLM-P75)
Contributions from cascade to the cross section for production of $He^+(2S)$. The semi-empirical cross section $Q_c^s(E)$ was calculated using equations (24a) and (24b)

The accuracy of this cascade cross section increases with increasing energy because the corrections to the plane-wave Born cross sections become progressively smaller.

9. RESULTS

It has been demonstrated previously that, at energies greater than fifteen or twenty times threshold, the absolute cross section for ionization of atomic hydrogen by electron impact (Fite and Brackmann 1958b) and the normalised cross sections for excitation to the 2P and 2S states (Fite and Brackmann 1958a and Stebbings, Fite, Hummer and Brackmann 1960) closely agree with the corresponding cross sections calculated using the plane-wave Born approximation. This is also true for the absolute cross section for ionization of He^+ (Dolder, Harrison and Thonemann 1961). At energies greater than about eight times threshold, the Coulomb potential of He^+ has very little effect and so the calculations at energies higher than this correspond to the plane-wave Born approximation. There is thus justification for normalising $Q_d(E)$ measured at the higher energies of this experiment

to $Q_p^{pb}(E) = Q_{1S \to 2S}^{pb}(E) + Q_c^s(E)$, given by the plane-wave Born approximation, in order to find $Q_p^e(E)$ over the entire energy range. When this procedure was applied it was found that $Q_p^e(E)$ could be made to agree very closely with $Q_p^{pb}(E)$ over the energy range 400 eV to 750 eV. The detector efficiency ε, which was discussed in Section 5, is equal to the reciprocal of the normalisation factor, and the value $\varepsilon = 6.77 \times 10^{-3}$ found in this way was within the limits of the value $\varepsilon = (8.3 \pm 2.5)\ 10^{-3}$ determined independently from the geometry and other properties of the detector as described in paper 1.

At energies near threshold, $C'(E)$, the count rate per unit beam currents due to the production of $He^+(2S)$ ions, was not directly related to the cross section $Q_p^e(E)$ because of the spread in energy of the electron beam. However, this energy distribution was measured and its effect was taken into account in order to determine the cross section from the measured count rate in the threshold region. The energy distribution was measured by a retarding potential method in which alternatively the plate d, the rear electron collector Ec‴, or the complete collector assembly d, Ec′, Ec″ and Ec‴ was biased. The average distribution obtained from many measurements made with the various biasing methods over a wide range of electron currents is shown in Fig. 10. Electron energies are shown relative to the mean electron energy E_m. The energy U_a[eV], corresponding to the accelerating potential between the cathode and anode of the electron gun, is also shown. The difference between these energies was estimated from the shape of the electron energy distribution and the value of U_a[eV] at which $C'(E)$ fell to zero. In fact E_m and U_a[eV] were found to coincide. Incident energies obtained in this manner were within the experimental limits of an independent estimate based upon the accelerating

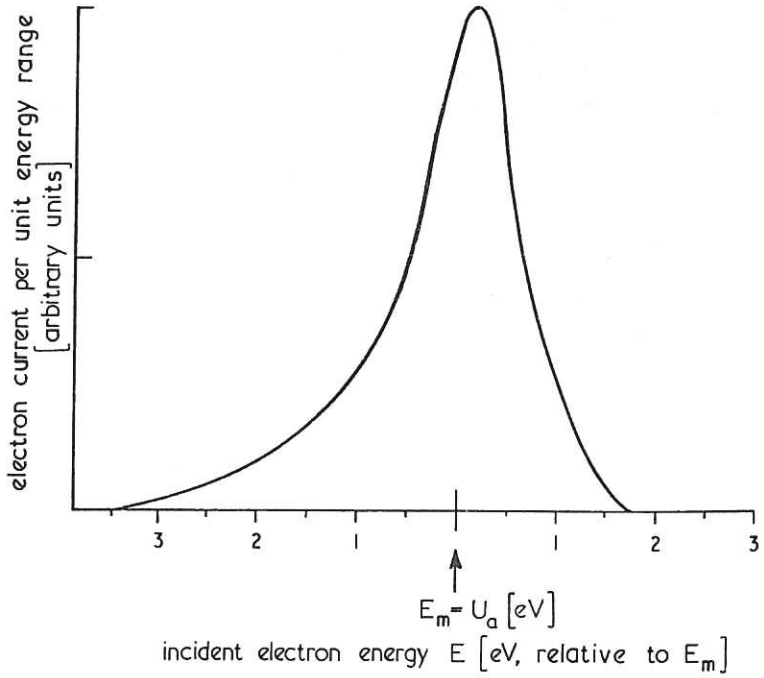

Fig. 10 (CLM-M75)
The electron energy distribution shown relative to the mean energy E_m. The energy U_a[eV] corresponding to the potential between the cathode and anode of the electron gun is also shown

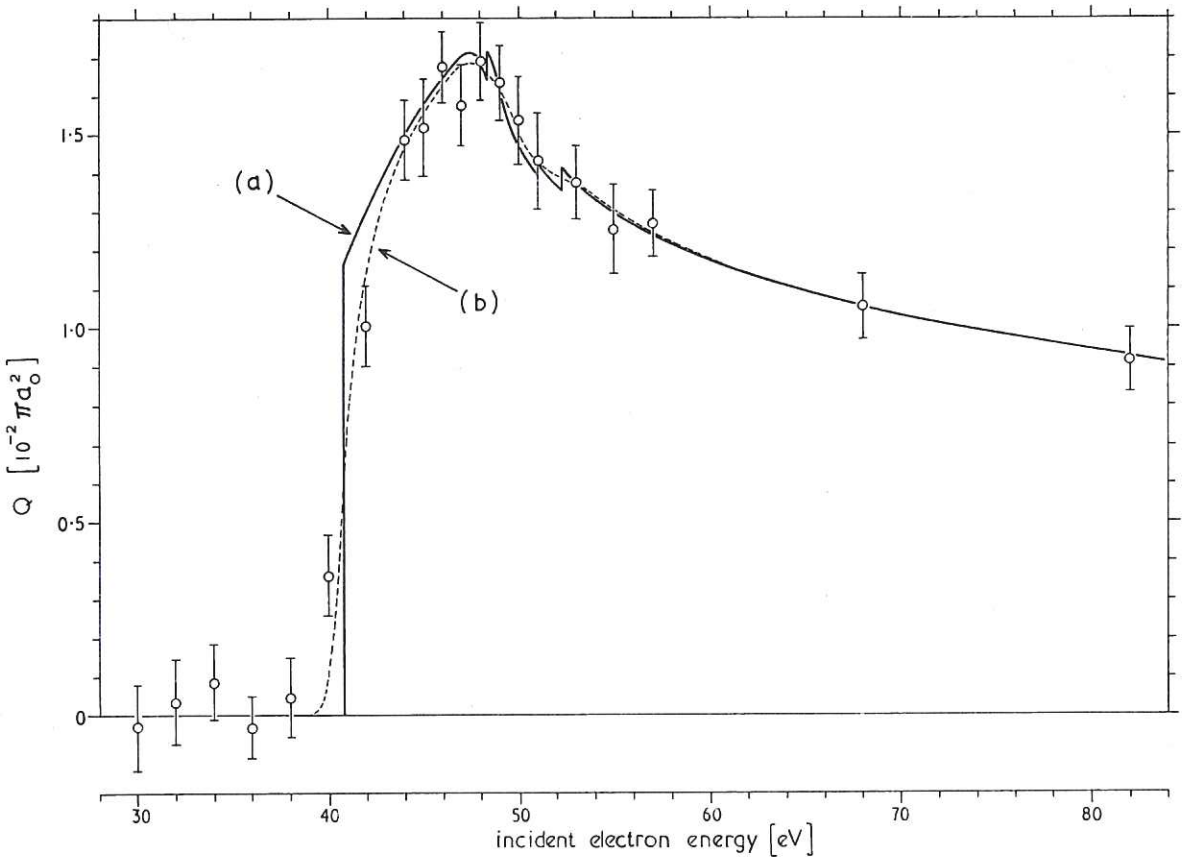

Fig. 11 (CLM-P 75)

The normalised cross section $Q_p^e(E)$ for the production of $He^+(2S)$ by electron impact excitation of $He^+(1S)$ at energies E near threshold. Curve (a) is $Q_p^e(E)$ and curve (b) is the overlap integral function O(E) plotted with E equal to the mean electron energy E_m. The normalised experimental points with 90% confidence limits are also plotted at their mean electron energies

potential U_a, the electron-ion relative velocity, the contact potential measured in the retarding potential experiments and the field penetration into the collision region. Uncertainties in the absolute energies obtained by the first method were about ± 0.5 eV.

The cross section $Q_p^e(E)$ near threshold has been estimated from the normalised values of C'(E) and electron energy distribution by a method of successive approximations. Computations were made at energies near threshold of the overlap integrals of the energy distribution and a trial cross section function. These overlap integrals should agree with C'(E) and so any disagreement was used to produce an improved trial cross section function. The cross section $Q_p^e(E)$ obtained in this manner is shown at energies near threshold as curve (a) of Fig. 11. The corresponding overlap integral function O(E) is shown as curve (b), which, at energies greater than 44 eV, is indistinguishable from a smooth curve drawn through the experimental points. The brackets indicate the 90% confidence limits of the points and it can be seen that the measurements at 40 eV and 42 eV do not quite agree with O(E). This discrepancy is attributed to small errors in the measured

electron energy distribution which were unimportant at higher energies. The electron energies given for curve (b) and for the experimental points are the mean energies E_m so that production of $He^+(2S)$ was still observed when the mean energy was slightly less than the threshold energy.

In Fig. 12 the normalised experimental results measured at energies greater than 55 eV are shown plotted at the mean electron energies. The error brackets once more represent 90% confidence limits. The absolute value of the cross section determined using the detector efficiency given in Section 5 is 0.82 ± 0.25 times the normalised cross section $Q_p^e(E)$. It is shown for clarity only at a single electron energy of 700 eV. The cross section

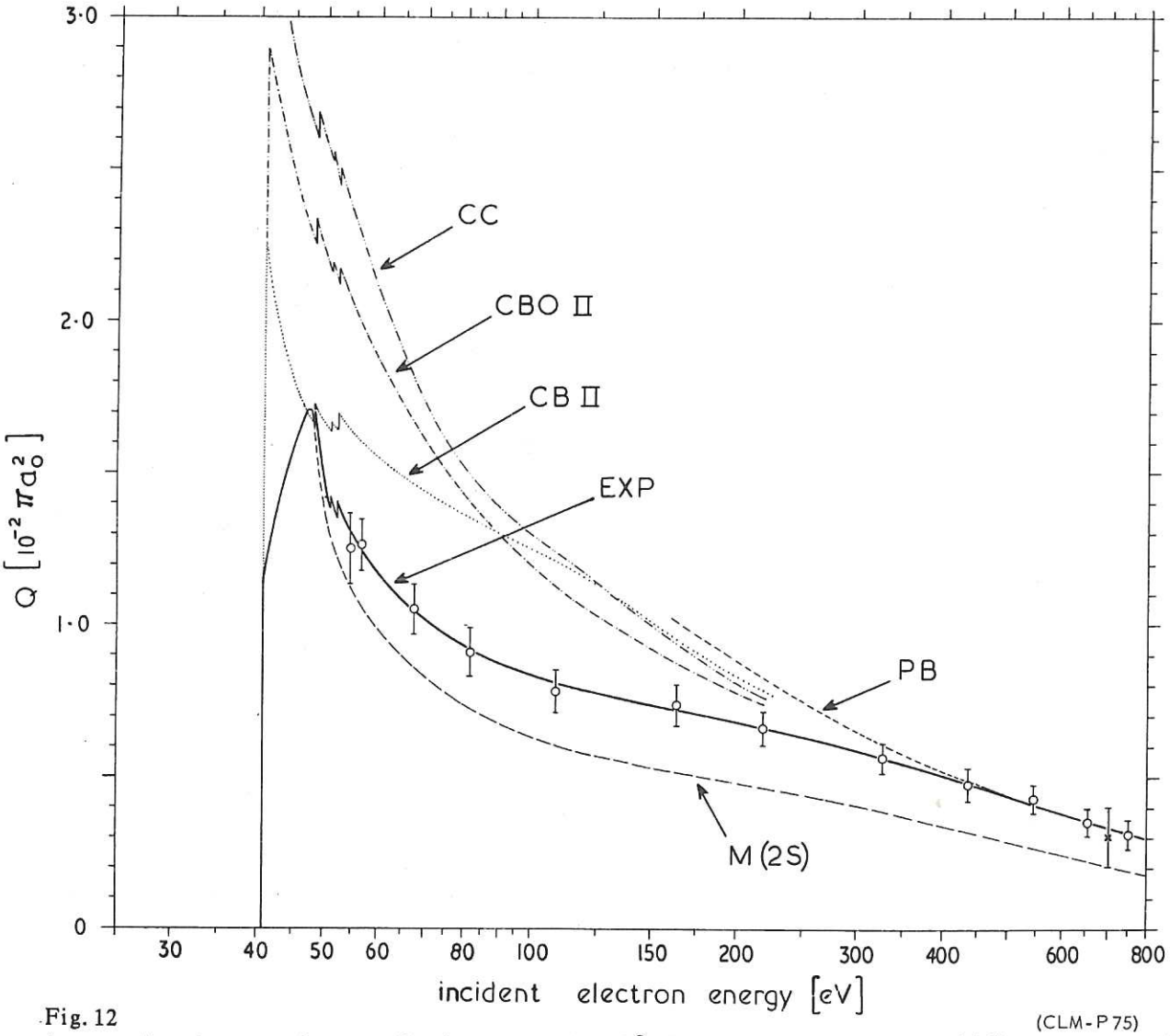

Fig. 12 (CLM-P75)

A comparison between the normalised cross section $Q_p^e(E)$ for the production of $He^+(2S)$ by electron impact excitation of $He^+(1S)$ and various theoretical cross sections $Q_p(E)$. Curve EXP shows $Q_p^e(E)$ found by normalisation to the plane-wave Born approximation (Massey 1956; curve PB). It is compared with cross sections given by the close-coupling approximation (Burke et al. 1964a; curve CC), by the Coulomb-Born approximation (Burgess et al. 1963; curve CB II) and by the Coulomb-Born-Oppenheimer approximation (Burgess et al. 1963; curve CBO II). The normalised experimental points with 90% confidence limits are plotted at their mean electron energies. The absolute value of the cross section determined using the detector efficiency given in paper 1 is shown by the cross and error brackets. For clarity this is plotted only at 700 eV. Curve M(2S) shows the experimentally determined cross section $Q^e_{1S \rightarrow 2S}(E)$ for the direct excitation to $He^+(2S)$

TABLE 1

(i)	(ii)	(iii)
electron energy E (eV)	cross section for production of $He^+(2S)$ $Q_p^e(E)$ $(10^{-2}\pi a_o^2)$	cross section for direct excitation of $He^+(2S)$ $Q_{1S\to 2S}^e(E)$ $(10^{-2}\pi a_o^2)$
40.8	0	0
2S threshold	1.17	1.17
44.0	1.49 ± 3.0%	1.49 ± 3.0%
46.0	1.65 ± 3.0%	1.65 ± 3.0%
47.4	1.71 ± 3.0%	1.71 ± 3.0%
48.4	1.64 ± 3.0%	1.64 ± 3.0%
3P threshold	1.72 ± 3.0%	
50.0	1.47 ± 3.0%	1.38
51.0	1.39 ± 3.0%	1.31
4P threshold	1.43 ± 3.0%	
52.2	1.35 ± 3.0%	1.24
5P threshold	1.41 ± 3.0%	
56.0	1.27 ± 3.5%	1.09
60.0	1.18 ± 4.0%	0.99
80.0	0.94 ± 4.0%	0.75
100	0.84 ± 4.0%	0.64
200	0.68 ± 4.0%	0.48
300	0.59 ± 4.0%	0.41
400	0.51 ± 4.0%	0.35
500	0.44 ± 4.5%	0.29
600	0.38 ± 4.5%	0.25
750	0.32 ± 4.5%	0.20

$Q_p^e(E)$ is shown by the curve labelled EXP and is compared with $Q_p(E)$ which has been determined by adding the cascade cross section $Q_c^s(E)$, as estimated in Section 8, to the cross sections $Q_{1S\to 2S}(E)$ calculated by several theoretical methods. These are the close-coupling approximation (Burke, McVicar and Smith 1964a; curve CC), the Coulomb-Born II approximation (Burgess, Hummer and Tully 1963; curve CB II) and the Coulomb-Born-Oppenheimer II approximation (Burgess, Hummer and Tully 1963; curve CBO II). These calculations have been extended to higher energies by the appropriately scaled plane-wave Born approximation cross sections for atomic hydrogen (Massey 1956; curve PB). The cross section $Q_{1S\to 2S}^e(E)$ for direct excitation to the 2S state of He^+ is the same as $Q_p^e(E)$ at energies lower than the 3P threshold, and at higher energies it was determined from the relationship

$$Q_{1S\to 2S}^e(E) = Q_p^e(E) - Q_c^s(E) \qquad \ldots (25)$$

and is shown by curve M(2S).

The results are also given in Table 1, in which column (i) gives the electron

energy, (ii) gives the cross section $Q_p^e(E)$ and (iii) gives the cross section $Q_{1S \to 2S}^e(E)$. Errors for $Q_p^e(E)$ were estimated from the root mean square deviation from $O(E)$ of all the experimental points including those at energies less than the threshold. Thus these errors represent the random errors of the experiment and take no account of errors introduced by normalisation. No errors are quoted at energies less than 44 eV because of possible error in the electron energy distribution function which would have a significant effect close to the threshold. At energies above the 3P threshold, the cross section $Q_{1S \to 2S}^e(E)$ is more uncertain than $Q_p^e(E)$ because of the semi-empirical method of estimating the cascade contributions.

10. DISCUSSION

The results of this experiment provide further evidence for the validity of the plane-wave Born approximation as applied to electron-ion collisions at high incident energies. In Fig. 12 it is seen that, at energies greater than ten times the threshold energy, the normalised cross section for production of $He^+(2S)$ varies with energy in the manner predicted by the plane-wave Born approximation, which includes cascade contributions. In addition the absolute magnitude of the cross section determined from the efficiency of the $He^+(2S)$ ion detector agrees with the magnitude given by the plane-wave Born approximation to well within the experimental uncertainty.

Agreement with theory becomes progressively worse towards lower energies, particularly from the threshold to 48 eV. Over this range the measured cross section increases with energy, but all the calculated cross sections show a decrease. At these energies the interpretation of the measurements is sensitive to the electron energy distribution, but if allowance were made for any other reasonable distribution the resulting cross section would still increase with energy in the first few electron volts above the threshold. It may be concluded that this experiment provides no evidence that the close-coupling approximation in its present form yields more accurate cross sections for $He^+(1S \to 2S)$ excitation than the Coulomb-Born type approximations. However, the measurements are consistent with a finite cross section at the threshold energy as predicted by all the theoretical methods.

11. ACKNOWLEDGEMENTS

We gratefully acknowledge the contributions made by Dr K.T. Dolder in the early stages of this experiment, and we also wish to thank R.R. Harrison and G.H. Hirst for their skilled assistance. We are indebted to Dr P.C. Thonemann for his advice and encouragement, and also the Director of the Culham Laboratory for his support of these investigations. We also thank Drs A. Burgess and P.G. Burke for their interest and for providing us with their results prior to publication.

12. REFERENCES

ACTON, F.S. 1959 Analysis of straight line data. New York: John Wiley and Sons Inc.

BURGESS, A. 1961 Mem. Soc. Roy. Sci. Liège, 4, 299.

BURGESS, A., HUMMER, D.G. and TULLY, J.A. 1963 Private communication. This work is discussed by Burke et al. (1964a).

BURKE, P.G., McVICAR, D.D. and SMITH, K. 1964a Proc. Phys. Soc. Lond., 83, 397.

BURKE, P.G., McVICAR, D.D. and SMITH, K. 1964b Proc. Phys. Soc. Lond., 84, 749.

CONDON, E.U. and SHORTLEY, G.H. 1959 The theory of atomic spectra, 136. Cambridge: University Press.

DOLDER, K.T., HARRISON, M.F.A. and THONEMANN, P.C. 1961 Proc. Roy. Soc.A, 264, 367.

FITE, W.L. and BRACKMANN, R.T. 1958a Phys. Rev., 112, 1151.

FITE, W.L. and BRACKMANN, R.T. 1958b Phys. Rev., 112, 1141.

HARRISON, M.F.A., DANCE, D.F., DOLDER, K.T. and SMITH, A.C.H. 1965 Rev. Sci. Instr., in course of publication (referred to as paper 1 in text).

HARRISON, M.F.A. 1965 Br. J. Appl. Phys., in course of publication (referred to as paper 2 in text).

HUMMER, D.G. and SEATON, M.J. 1961 Phys. Rev. Lett., 6, 471.

HUMMER, D.G. 1963 Ph.D. thesis. University of London.

LAMB, W.E. and SKINNER, M. 1950 Phys. Rev., 78, 539.

LICHTEN, W. and SCHULTZ, S. 1959 Phys. Rev., 116, 1132.

LICHTEN, W. 1961 Phys. Rev. Lett., 6, 12.

MASSEY, H.S.W. 1956 Encyclopedia of physics, 36, 354. Berlin: Springer-Verlag.

SEATON, M.J. 1962 Atomic and molecular processes (edited by D.R. Bates), 374. New York: Academic Press.

STEBBINGS, R.F., FITE, W.L., HUMMER, D.G. and BRACKMANN, R.T. 1960 Phys. Rev., 119, 1939. See also FITE, W.L. 1962 Atomic and molecular processes (edited by D.R. Bates), 451. New York: Academic Press.

TULLY, J.A. 1960 M.Sc. dissertation. University of London. See also Seaton (1962).